Talanta 87 (2011) 189–196

Contents lists available at SciVerse ScienceDirect

Talanta

journal homepage: www.elsevier.com/locate/talanta

Amperometric biosensors based on deposition of gold and platinum nanoparticles on polyvinylferrocene modified electrode for xanthine detection

Salih Zeki Baş[a,*], Handan Gülce[b], Salih Yıldız[a], Ahmet Gülce[b]

[a] Department of Chemistry, Selcuk University, Konya, Turkey
[b] Department of Chemical Engineering, Selcuk University, Konya, Turkey

ARTICLE INFO

Article history:
Received 8 July 2011
Received in revised form
20 September 2011
Accepted 27 September 2011
Available online 1 October 2011

Keywords:
Amperometric biosensor
Xanthine oxidase
Xanthine detection
Gold deposition
Platinum deposition
Polyvinylferrocene

ABSTRACT

In this study, new xanthine biosensors, XO/Au/PVF/Pt and XO/Pt/PVF/Pt, based on electroless deposition of gold(Au) and platinum(Pt) nanoparticles on polyvinylferrocene(PVF) coated Pt electrode for detection of xanthine were presented. The amperometric responses of the enzyme electrodes were measured at the constant potential, which was due to the electrooxidation of enzymatically produced H_2O_2. Compared with XO/PVF/Pt electrode, XO/Au/PVF/Pt and XO/Pt/PVF/Pt exhibited excellent electrocatalytic activity towards the oxidation of the analyte. Effect of Au and Pt nanoparticles was investigated by monitoring the response currents at the different deposition times and the different concentrations of $KAuCl_4$ and $PtBr_2$. Under the optimal conditions, the calibration curves of XO/Au/PVF/Pt and XO/Pt/PVF/Pt were obtained over the range of 2.5×10^{-3} to 0.56 mM and 2.0×10^{-3} to 0.66 mM, respectively. The detection limits were 7.5×10^{-4} mM for XO/Au/PVF/Pt and 6.0×10^{-4} mM for XO/Pt/PVF/Pt. The effects of interferents, the operational and the storage stabilities of the biosensors and the applicabilities of the proposed biosensors to the drug samples analysis were also evaluated.

1. Introduction

Xanthine oxidase catalyzes the oxidation of hypoxanthine to xanthine and of xanthine to uric acid. Thus, XO plays an important role in the catabolism of purines in human and mammalian life [1,2]. The determination of xanthine level is required in food industries for the quality control of fish products and in blood and tissue samples for the diagnosis and the treatment of various diseases like gout, xanthinuria and hyperuricaemia [3]. In the literature, several analytical methods such as enzymic colorimetric [4], electrophoresis [5,6], capillary column gas chromatography [7], HPLC [8,9] have been reported for the determination of xanthine. However, these methods are time-consuming, difficult, expensive and requires sample preparation. XO-based electrochemical biosensors have been frequently used for the determination of xanthine [10–13]. Generally, the electrochemical detection of xanthine is based on the electrochemical oxidation of the enzymatically generated H_2O_2, or the electrochemical reaction of the introduced redox mediators [14]. Compared with other analytical methods, enzyme-based electrochemical sensors possess simplicity of operation, high sensitivity and selectivity. In addition to these features, the sensors have advantages such as its ease of use in turbid samples, portability, low cost and fast [15,16].

Metal particles used as electrode modified materials have attracted much attention in the electrochemical applications, recently [17–20]. The previous studies indicated that gold and platinum nanoparticles could increase the surface area and conducive to electron transfer with strong catalytic properties [21–23]. For example, Zou et al. [24] reported a novel glucose biosensor based on electrodeposition of platinum nanoparticles onto multi-walled carbon nanotube, and the prepared biosensor exhibited excellent electrocatalytic activity towards H_2O_2 electrooxidation and high stability. Du et al. [25] fabricated a new glucose biosensor based on the film of chitosan-gold nanoparticles, and observed a remarkable increase in the oxidation current. Chu et al. [26] developed a new amperometric biosensor based on adsorption of glucose oxidase at the gold and platinum nanoparticles modified carbon nanotube electrode, and the enzyme electrode exhibited good catalytic activity to the electrooxidation of H_2O_2.

Polyvinylferrocene (PVF) is an example of a redox polymer that contains localized sites which may be oxidized and reduced [27]. PVF is widely used as a excellent electron transfer mediator in the electrochemical systems because of the advantages of simple electrochemistry (a reversible one-electron process), high stability and the ease of coating of thin films using a variety of methods [28]. It was observed that PVF has attracted interest with regard to the applications as electrocatalysis for the electroreduction and the electrooxidation of anthracene and some of its derivatives [29,30] and the electrooxidation of hydrogen peroxide [31]. In addition, the previous studies indicated that the metal nanoparticles could be

* Corresponding author. Tel.: +90 3322233877.
E-mail address: salihzekibas@gmail.com (S.Z. Baş).

0039-9140/$ – see front matter © 2011 Elsevier B.V. All rights reserved.
doi:10.1016/j.talanta.2011.09.060

deposited chemically on the PVF coated electrode surface without the application of any potential [32]. The performance of the modified PVF film for the biosensing applications was demonstrated. For example, Gülce et al. [33] developed a new glucose biosensor based on the electroless deposition of gold nanoparticles on the PVF film, and the prepared biosensor exhibited excellent electrocatalytic activity to the electrooxidation of H_2O_2. During immersion of the electrode into the gold solution in the deposition process, the chemical reduction occurred according to the following reaction,

$$3PVF + AuX_4^- \rightarrow 3PVF^+ + Au + 4X^-$$

As a result of this alternative possibility to deposit gold on the PVF coated electrode, we investigated the electroless deposition of platinum on the PVF film without the application of any potential, and observed that metallic platinum could be easily deposited on the PVF coated electrode by means of the chemical reduction of platinum ion by PVF. Thus, new xanthine biosensors based on the electroless deposition of gold and platinum nanoparticles on PVF coated Pt electrodes were constructed. The experimental conditions related to the preparation and the characterization of the biosensors were studied in detail. The changes in the responses of the enzyme electrodes with various parameters such as applied potential, polymeric film thickness, deposition time of Au and Pt nanoparticles, $KAuCl_4$ concentration, $PtBr_2$ concentration, substrate and enzyme concentrations and temperature were established. The performances of the biosensors, i.e. linear range, sensitivity, response time and stability were also described. In addition, the proposed biosensors were applied to the analysis of the drug samples containing xanthine derivatives.

2. Experimental

2.1. Reagents

PVF was prepared using a method of chemical polymerization [34] of vinylferrocene (Alfa Aesar, Ward Hill, MA, USA). The purification of methylene chloride (Merck, Darmstadt, Germany) was accomplished according to the method proposed in literature [35]. Xanthine oxidase (EC 1.17.3.2, Fluka-86106) and xanthine (Fluka-X0626) were purchased from Sigma (St. Louis, MO, USA). Phosphate buffer solution (PBS) was prepared using NaH_2PO_4 (Merck, Darmstadt, Germany) and NaOH (Merck, Darmstadt, Germany). The enzyme solution was prepared by dissolving of XO in 0.01 M PBS of pH 7.4, and stored at 4 °C. Xanthine solution was prepared in 0.1 M PBS of pH 7.4. $KAuCl_4$ solution was prepared by dissolving $KAuCl_4$ (St. Louis, MO, USA) in 0.01 M KCl (Merck, Darmstadt, Germany) solution. $PtBr_2$ solution was prepared by dissolving $PtBr_2$ (St. Louis, MO, USA) in 0.01 M HBr (Merck, Darmstadt, Germany) solution. All aqueous solutions were prepared in deionized water.

2.2. Apparatus and instrumentations

All the electrochemical measurements were performed with a CHI-660C electrochemical workstation (Shanghai CH Instruments Co., China). A conventional three electrode system was used with platinum electrode (area: 0.0314 cm^2) as working electrode, a platinum wire as auxiliary electrode, and an Ag/AgCl (3 M KCl) electrode as reference electrode. Prior to each experiment, Pt electrode was polished with 1.0, 0.3 and 0.05 μm alumina powder, then ultrasonicated in methylene chloride and twice-deionized water, respectively. Scanning electron microscopy (SEM) and atomic force microscopy (AFM) images were obtained by using EVO-LS 10 (Carl Zeiss, Germany) and NTEGRA (NT-MDT, Russia).

2.3. Preparation of the enzyme electrodes

The Pt electrode was immersed in a solution of PVF (5.0 mg mL^{-1}) in methylene chloride and the solvent was then evaporated for the preparation of the PVF coated Pt electrode (PVF/Pt). The average thickness of the dry film was estimated from the charge consumed during complete electrooxidation of the film by stepping the potential from 0.0 to 0.7 V versus SCE in 0.1 M PBS as described by Bard [36]. The PVF coated Pt electrode was immersed in $KAuCl_4$ solution (the optimal concentration: 2.0 mM) for some time (the optimal deposition time: 2 min) without the application of any potential for the preparation of gold deposited PVF coated Pt electrode (Au/PVF/Pt). Pt/PVF/Pt electrode was prepared by deposition of platinum on the PVF coated Pt electrode in $PtBr_2$ solution (the optimal concentration: 1.5 mM, the optimal deposition time: 10 min) using the same procedures above. Au/PVF/Pt and Pt/PVF/Pt electrodes were kept in the enzyme solution without stirring for 20 min during the immobilization of XO. The enzyme electrodes (XO/Au/PVF/Pt and XO/Pt/PVF/Pt) were rinsed with buffer solution to remove the enzyme not immobilized, and then stored at 4 °C in 0.01 M PBS prior to use. The procedure for preparing the enzyme electrodes are schematically shown in Scheme 1. For comparison, XO/PVF/Pt electrode without Au and Pt nanoparticles was fabricated using the procedure as described above.

3. Results and discussion

3.1. SEM images, AFM images and cyclic voltammograms of the enzyme electrodes

The determination of xanthine based on the electrochemical oxidation of enzymatically generated H_2O_2 has been successfully applied to the process of the immobilized electrodes [37–40]. In consideration of the electrodes prepared with XO enzymes, the biocatalytical process for the oxidation of xanthine in the presence of XO can be summarized as following process.

The immobilized enzyme produces electroactive H_2O_2 as a result of following reaction with xanthine,

$$\text{xanthine} + O_2 + H_2O \xrightarrow{XO} \text{uric acid} + H_2O_2$$

H_2O_2 could be electrooxidized at the applied potential according to

$$H_2O_2 \rightarrow O_2 + 2H^+ + 2e^-$$

Fig. 1 shows the typical cyclic voltammograms of XO/PVF/Pt (a), XO/Au/PVF/Pt (b), XO/Pt/PVF/Pt (c) electrodes in the absence and the presence of xanthine in 0.1 M PBS (pH 7.4) at scan rate of 50 mV s^{-1}. When xanthine (0.20 mM for XO/PVF/Pt, 0.40 mM for XO/Au/PVF/Pt and XO/Pt/PVF/Pt) was added into PBS, the cyclic voltammograms of the enzyme electrodes display the oxidation peaks between +0.7 V and +0.4 V due to the electrooxidation of enzymatically produced H_2O_2. The peak current values obtained with XO/Au/PVF/Pt (Fig. 1b, curve 2) and XO/Pt/PVF/Pt (Fig. 1c, curve 2) electrodes were substantially higher than that obtained with XO/PVF/Pt electrode (Fig. 1a, curve 2), indicating that Au and Pt nanoparticles play an important role in increasing the electroactive surface area of the electrodes. Furthermore, the oxidation peak potentials of XO/Au/PVF/Pt and XO/Pt/PVF/Pt electrodes shifted to less positive potential due to the high catalytic activity of Au and Pt nanoparticles. These results were in agreement with that reported for metal particles-based electrodes [33,41,42].

Fig. 2 shows the SEM images of the enzyme electrodes, XO/PVF/Pt (a), XO/Au/PVF/Pt (b), XO/Pt/PVF/Pt (c), and the modified electrodes, PVF/Pt (inset a), Au/PVF/Pt (inset b), Pt/PVF/Pt (inset c). As shown in Fig. 2(inset a), the polymer film has suitable

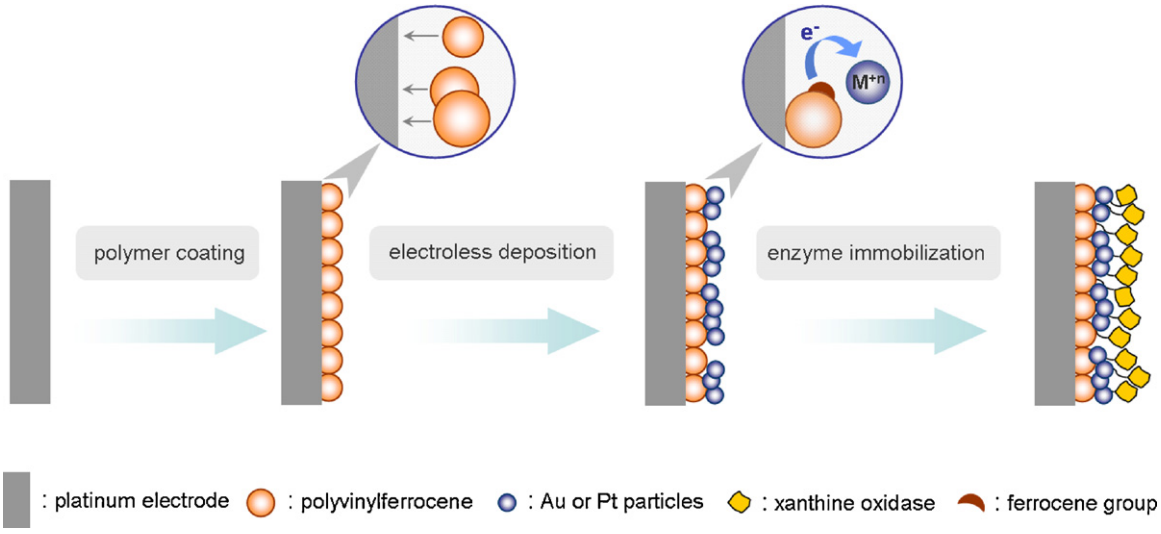

Scheme 1. Schematic representation of constructions of XO/Pt/PVF/Pt and XO/Au/PVF/Pt.

surface area which provides an ideal matrix for the metal deposition and the immobilization of enzyme. As XO was immobilized on the PVF film, the SEM image of the XO/PVF/Pt (Fig. 2a) showed a heterogeneous morphology and formed a covered surface. From Fig. 2(insets b and c), it can be seen Au and Pt nanoparticles are dispersed well on the polymer surface. Pt particles, with a diameter ranging from 50 nm to 150 nm, are distributed more densely and larger size than that in Fig. 2(inset b). The size of Au particles is about 40–100 nm. The SEM images of XO/Au/PVF/Pt (Fig. 2b) and XO/Pt/PVF/Pt (Fig. 2c) showed a significant difference when compared to that of XO/PVF/Pt with no deposited metal particles (Fig. 2a), revealing the high enzyme loading of these two electrodes. The enzyme was attached to the entire surfaces of Au/PVF/Pt and Pt/PVF/Pt, indicating the successful immobilization of XO.

The topographical analysis of PVF film, Au deposited PVF film and Pt deposited PVF film was also performed using AFM and the surface images were shown three-dimensionally in Fig. 3. Fig. 3a is a typical AFM image of the PVF film surface. It shows a smooth fractal behavior. Root mean square (RMS) roughness of the PVF film is 56 nm for a 5 μm × 5 μm area. Fig. 3b shows the AFM image of electrolessly deposited Au nanoparticles on the PVF film. The Au nanoparticles have a size of about 90 nm, and are randomly distributed on the polymer surface. After the deposition of Au nanoparticles, the RMS value of the modified film increased to

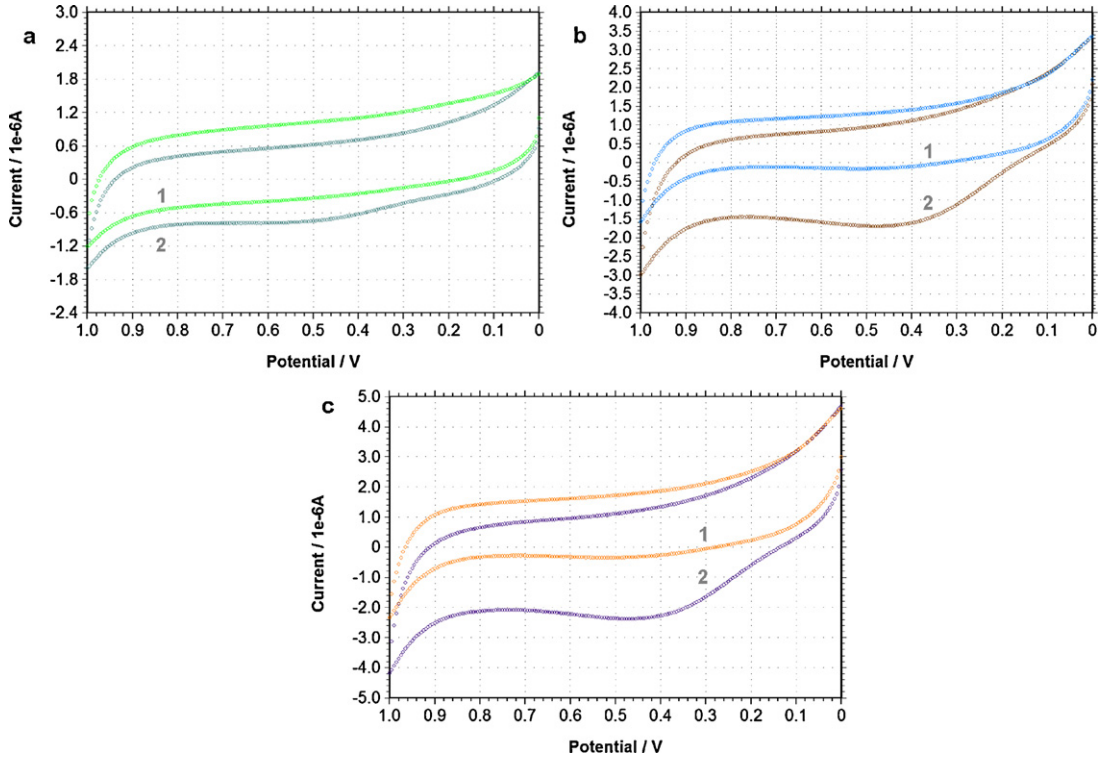

Fig. 1. Cyclic voltammograms of XO/PVF/Pt (a), XO/Au/PVF/Pt (b) and XO/Pt/PVF/Pt (c) in the absence (1) and presence (2) of xanthine (0.20 mM for XO/PVF/Pt, 0.40 mM for XO/Au/PVF/Pt and XO/Pt/PVF/Pt) in 0.1 M PBS (pH 7.4).

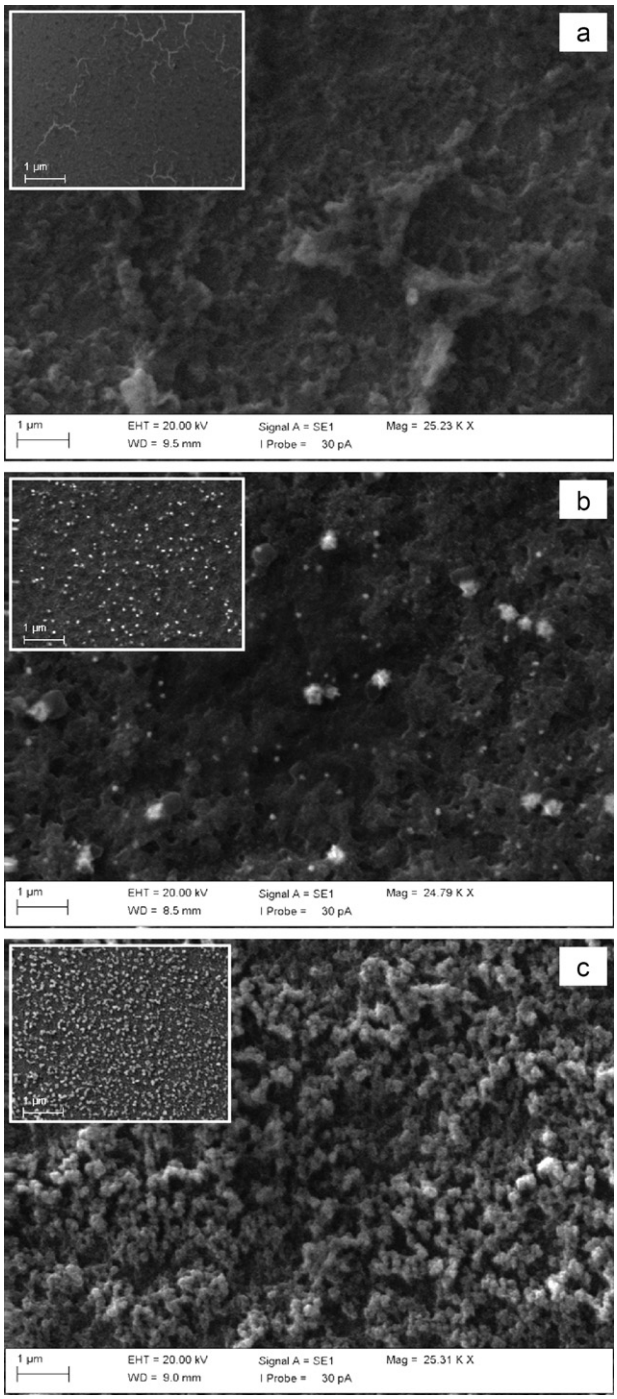

Fig. 2. SEM images of the enzyme electrodes, XO/PVF/Pt (a), XO/Au/PVF/Pt (b), XO/Pt/PVF/Pt (c), and the modified electrodes, PVF/Pt (inset a), Au/PVF/Pt (inset b), Pt/PVF/Pt (inset c).

79 nm, which confirmed gold ion was effectively reduced to metallic gold. Fig. 3c exhibits the AFM image of the PVF film modified with Pt nanoparticles. The size of Pt nanoparticles is about 120 nm, and the RMS value is 97 nm, which is larger than that of Fig. 1a. As can be seen in the figure, Pt nanoparticles are obviously formed on the PVF film, which manifested that platinum ion can be reduced to metallic platinum without the application of any potential.

3.2. Effect of polymeric film thickness

The effect of the thickness of PVF film on the Pt electrode surface was investigated in the thicknesses of PVF film ranging between 1.1×10^{-7} mol cm^{-2} of PVF (dry thickness ~0.24 μm) and 5.5×10^{-7} mol cm^{-2} of PVF (dry thickness ~1.20 μm). The response current increased with the polymer thickness up to a value corresponding to 3.8×10^{-7} mol cm^{-2} of PVF (dry thickness ~0.82 μm) and then, the response current decreased slowly with increasing film thickness. The thickness of PVF film was kept constant at this value for all measurements.

3.3. Effects of XO concentration

The enzyme amount in the polymer matrix depends on the concentration of XO in solution used during immobilization process. The effect of the enzyme amount on the response current was investigated in the enzyme concentrations varying between 0.5 and 8.0 mg mL^{-1} to decide on the optimal amount. When the concentration of XO was higher than 2.0 mg mL^{-1}, the response current did not change appreciably. The enzyme concentration of 2.0 mg mL^{-1} was used for constructing the enzyme electrodes in all of measurements.

3.4. Effect of applied potential

The effect of applied potential on the response currents of the enzyme electrodes was examined amperometrically at different potentials between 0.2 and 0.8 V. The maximum response currents of XO/PVF/Pt, XO/Au/PVF/Pt and XO/Pt/PVF/Pt electrodes were obtained at potentials of 0.65 V, 0.4 V and 0.4 V versus SCE, respectively. These results obtained are consistent with the results of the cyclic voltammograms, indicating that the response current of the enzyme electrodes is based on the electrochemical oxidation of enzymatically formed H_2O_2.

3.5. Effect of deposition time and concentration of $KAuCl_4$ and $PtBr_2$

The amounts of Au and Pt nanoparticles on the polymer film depend on the concentrations of $KAuCl_4$ and $PtBr_2$ used during deposition process. The effects of the different concentrations of $KAuCl_4$ and $PtBr_2$ on the response current were investigated and the corresponding results were shown in Fig. 4a and b. The maximum current values were obtained from XO/Au/PVF/Pt and XO/Pt/PVF/Pt electrodes prepared using 2.0 mM $KAuCl_4$ and 1.5 mM $PtBr_2$, respectively. Furthermore, the effect of the deposition time Au and Pt nanoparticles on the response current of the enzyme electrodes was investigated. From Fig. 4c and d, it can be observed that the response currents of XO/Au/PVF/Pt and XO/Pt/PVF/Pt electrodes are affected obviously by the loading mass of Au and Pt nanoparticles. The optimal deposition time of XO/Au/PVF/Pt and XO/Pt/PVF/Pt was found to be 2 min and 10 min, respectively. All these results may be attributed that the increase of the deposition time and the metal concentration decreased the electrochemical active surface area of the electrode because of the large-sized nanoparticles and affected negatively to electrocatalytic activity [19,33,43].

3.6. Effect of temperature

The effect of temperature on the response currents of XO/Au/PVF/Pt and XO/Pt/PVF/Pt electrodes was investigated at the different temperatures ranging from 20 to 55 °C. For both enzyme electrodes, the response current, which correspond the activity of the immobilized XO, increased with increasing temperature from 20 to 40 °C, and then decreased after this temperature. The decrease in the response currents of the enzyme electrodes at a higher temperature may have two reasons: one is the decreasing concentration of molecular oxygen in the solution, another is the thermal

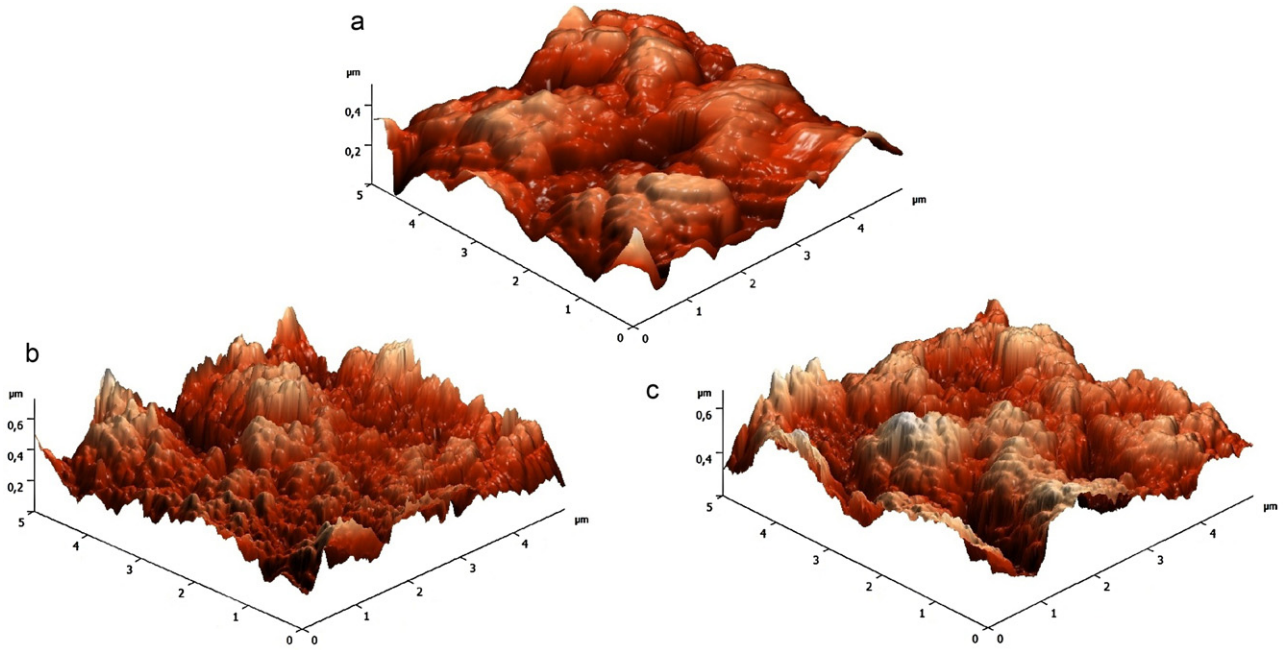

Fig. 3. AFM images of the modified electrodes, PVF/Pt (a), Au/PVF/Pt (b), and Pt/PVF/Pt (c).

deactivation of the enzyme at higher temperatures [44]. In addition, the response current of XO/PVF/Pt (without Au and Pt nanoparticles) were tested at different temperatures between 20 and 55 °C, and reached a maximum at 35 °C. This result showed that stability of the immobilized enzyme was increased slightly by the deposition of Au and Pt.

The temperature effect on the amperometric current can be described by the Arrhenius equation (1) [45]:

$$i(T) = i_0 \exp\left(-\frac{E_a}{RT}\right) \quad (1)$$

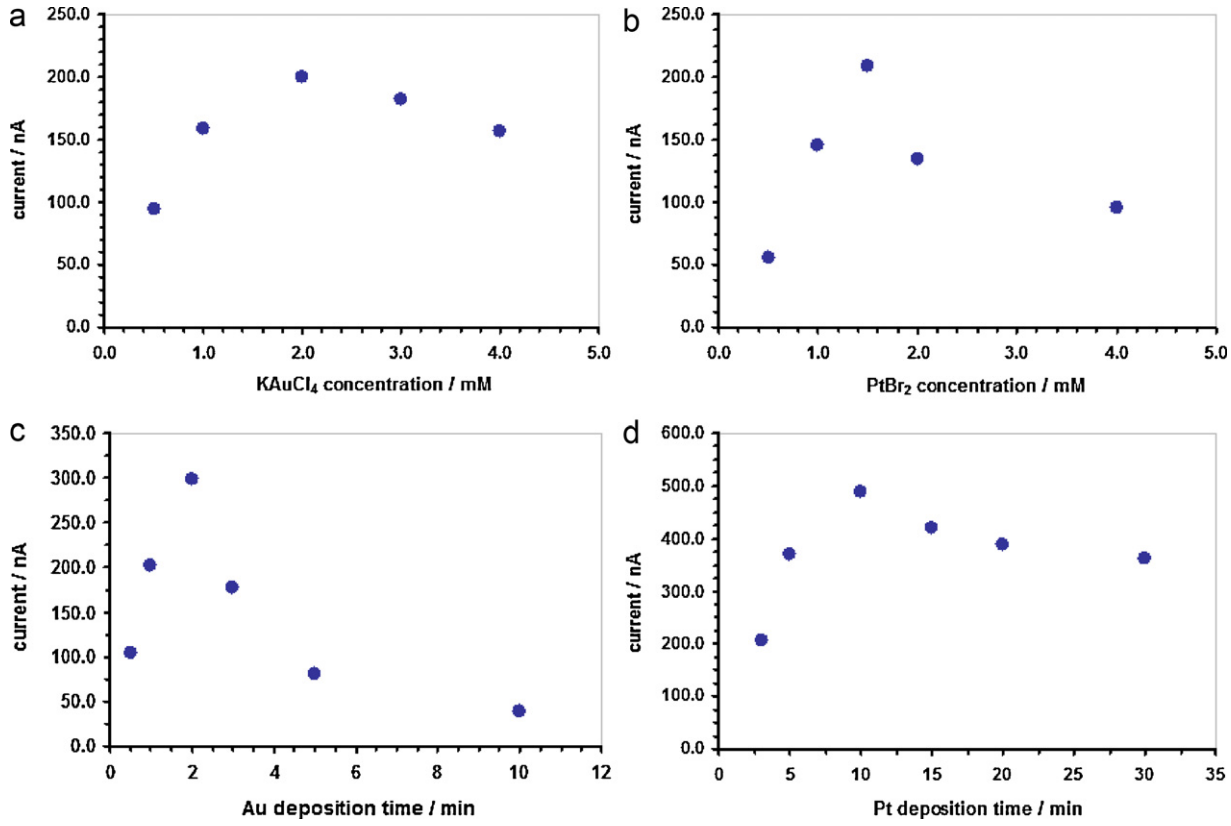

Fig. 4. The effect of the concentration of $KAuCl_4$ (a) and $PtBr_2$ (b), the deposition time of Au (c) and Pt (d) nanoparticles on the response current in 0.1 M PBS (pH 7.4) at the applied potential of 0.4 V.

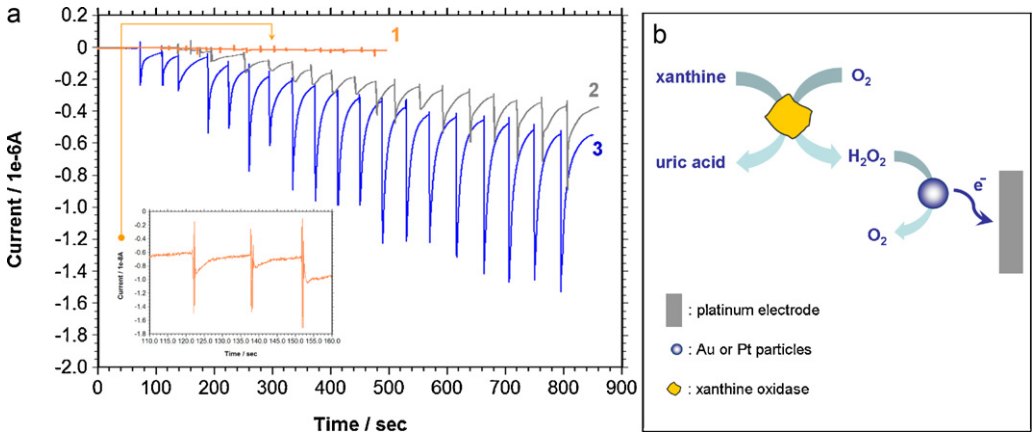

Fig. 5. (a) Amperometric response of XO/PVF/Pt (1), XO/Au/PVF/Pt (2) and XO/Pt/PVF/Pt (3) with successive addition of 2.0×10^{-2} M xanthine in 0.1 M PBS (pH 7.4) at the applied potential of 0.65 V (1), 0.40 V (2 and 3). (b) The mechanism of amperometric xanthine detection.

where i_0 is a collection of currents, i is the steady-state current, E_a is the activation energy, R is the universal gas constant and T is the absolute temperature in K. The E_a values for the oxidation of xanthine on XO/Au/PVF/Pt and XO/Pt/PVF/Pt electrodes were found to be 18.28 kJ mol^{-1} and 20.36 kJ mol^{-1} from the slope of the plot of ($\ln i - 1/T$) in the appropriate region of temperature.

3.7. Amperometric responses of the enzyme electrodes

Fig. 5a shows the current–time curves for XO/PVF/Pt (1), XO/Au/PVF/Pt (2) and XO/Pt/PVF/Pt (3) upon the successive addition of the different concentrations of xanthine in a stirred buffer solution under the optimal conditions. Inset of Fig. 5a displays a part of the typical amperometric response of XO/PVF/Pt electrodes. Apparently, low amperometric responses observed at XO/PVF/Pt electrode compared with the remarkable current staircases at XO/Au/PVF/Pt and XO/Pt/PVF/Pt electrodes after each addition of xanthine, indicating the effective electron-transfer ability of Au and Pt nanoparticles towards oxidation of the enzymatically formed H_2O_2 (Fig. 5b). Both xanthine biosensors reached 90% of the steady-state current within 15–20 s. But, the amperometric response signal of XO/Pt/PVF/Pt electrode is a bit larger than that of XO/Au/PVF/Pt.

Fig. 6a and b shows the changes in the response currents of XO/Au/PVF/Pt and XO/Pt/PVF/Pt electrodes as a function of xanthine concentration. The response current of XO/Au/PVF/Pt electrode is linear in the range from 2.5×10^{-3} to 0.56 mM with a correlation coefficient of 0.9949 (Fig. 6c). Compared with XO/Au/PVF/Pt electrode, XO/Pt/PVF/Pt electrode exhibits a wider linear range from 2.0×10^{-3} to 0.66 mM with a correlation coefficient of 0.9966 (Fig. 6d). These results are better than those of previous biosensors based on polypyrrole-ferrocenium coated platinum electrode (1.0×10^{-2} to 0.4 mM) [46] and nano-$CaCO_3$ modified electrode (2.0×10^{-3} to 0.25 mM) [15] but lower than that of β-cyclodextrin-branched carboxymethylcellulose modified gold electrode (0.3–10.4 mM) [11]. The detection limits of XO/Au/PVF/Pt and XO/Pt/PVF/Pt were 7.5×10^{-4} mM and 6.0×10^{-4} mM at the signal-to-noise ratio of 3 (S/N = 3), respectively, which are lower than that of ZnO-NPs-polypyrrole composite film (8.0×10^{-4} mM) [13], nano-$CaCO_3$ modified electrode (2.0×10^{-3} mM) [15], polypyrrole-ferrocenium coated platinum electrode (1.0×10^{-3} mM) [46], but higher than multi-wall carbon nanotubes modified glassy carbon electrode (1.0×10^{-4} mM) [12], laponite thin film modified electrode (1.0×10^{-5} mM) [14]. The current sensitivities are 28.95 μA mM^{-1} cm^{-2} and 53.08 μA mM^{-1} cm^{-2} to xanthine

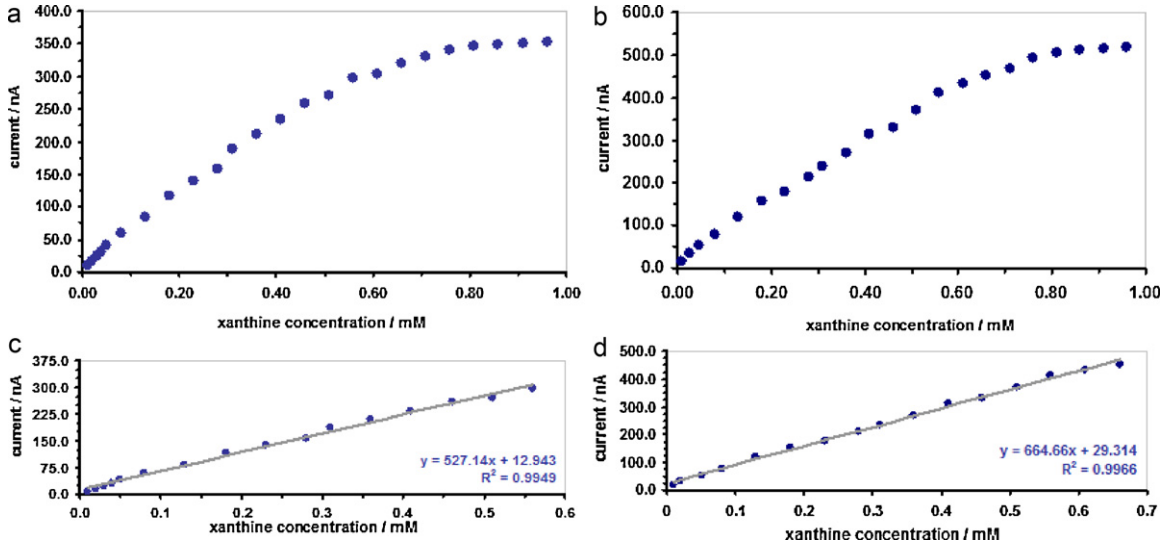

Fig. 6. The change in the response currents of XO/Au/PVF/Pt (a) and XO/Pt/PVF/Pt (b) with successive addition of xanthine and the calibration curves of XO/Au/PVF/Pt (c) and XO/Pt/PVF/Pt (d) in 0.1 M PBS (pH 7.4) at the applied potential of 0.4 V.

Table 1
Results of the xanthine assay in the drug samples using XO/Au/PVF/Pt (A) and XO/Pt/PVF/Pt (B).

Biosensor	Drug sample	Given by prospectus (mM)	Xanthine added (mM)	Determined by the biosensor[a] (mM)	Recovery (%)
A	1	0.114	0	0.112 ± 0.010	–
			0.200	0.303 ± 0.019	95.5
	2	0.083	0	0.082 ± 0.012	–
			0.200	0.271 ± 0.019	94.5
B	1	0.114	0	0.120 ± 0.014	–
			0.200	0.310 ± 0.017	95.0
	2	0.083	0	0.076 ± 0.012	–
			0.200	0.265 ± 0.017	94.5

[a] Average of three determinations ± standard deviation.

for XO/Au/PVF/Pt and XO/Pt/PVF/Pt electrodes, respectively. The apparent Michaelis–Menten constant ($K_{m_{app}}$) can be calculated from the electrochemical version of the Linweaver–Burk equation (2) [47]:

$$\frac{1}{i_s} = \frac{1}{i_{max}} + \left(\frac{K_{m_{app}}}{i_{max}}\right)\left(\frac{1}{C}\right) \quad (2)$$

where i_s is the steady-state current, i_{max} is the maximum current, $K_{m_{app}}$ the apparent Michaelis–Menten constant, C is the concentration of xanthine. The $K_{m_{app}}$ values were found to be 0.393 mM and 0.286 mM for XO/Au/PVF/Pt and XO/Pt/PVF/Pt, respectively. The $K_{m_{app}}$ values of the biosensors are smaller than those of reported in the literature [11,46]. The smaller $K_{m_{app}}$ values meant that XO immobilized on the modified PVF film exhibited high enzymatic activity and affinity to xanthine.

3.8. Reproducibility and stability

The reproducibility of both enzyme electrodes, XO/Au/PVF/Pt and XO/Pt/PVF/Pt, was estimated from the response to 0.30 mM xanthine for five enzyme electrodes prepared under the optimal conditions and the relative standard deviation (R.S.D.) is 3.41% for XO/Au/PVF/Pt and 4.70% for XO/Pt/PVF/Pt. The storage stability of XO/Au/PVF/Pt and XO/Pt/PVF/Pt electrodes was also studied. The storage stability of the enzyme electrodes was determined by measuring steady-state response current of 0.30 mM xanthine during 30 days. When not in use, the enzyme electrodes were kept in 0.01 M PBS (pH 7.4) at 4 °C. The XO/Au/PVF/Pt electrode exhibited good stability during 10 days. The response current remained about 90% of its initial response and then, an activity loss of 40% was observed on the 18th day. The lifetime of XO/Pt/PVF/Pt electrode was slightly longer than the XO/Au/PVF/Pt electrode and the response current of XO/Pt/PVF/Pt on the 14th days was 90% of the initial value. After 23 days, the response current lost 40% of its initial response.

3.9. Interference study

The effect of possible interfering substances on XO/Au/PVF/Pt and XO/Pt/PVF/Pt electrodes was investigated by using ascorbic acid and uric acid at 0.4 V (versus SCE) in 0.1 M PBS (pH 7.4). The response currents obtained in the presence of the interfering species (0.1 mM ascorbic acid, 0.2 mM uric acid) were compared with the xanthine response obtained for 0.4 mM xanthine solution. No appreciable signals were observed for the addition of the uric acid solution into the electrolyte solution. It was found that the presence of ascorbic acid have the current value of 17.2% for XO/Au/PVF/Pt and 20.5% for XO/Pt/PVF/Pt when the xanthine response is taken as 100%. Typically, Nafion, a perfluorosulfonate cation-exchange polymer, is used to remove the interfering signal from the electroactive species such as ascorbic acid, uric acid. At the pH of 7.4, ascorbic acid (pK_a = 4.17) and uric acid (pK_a = 5.27) exist in anionic form. Thus, a Nafion-coated surface repulses anionic ascorbic acid and uric acid, and allows the movement of the target cationic species. We applied this method to our electrodes by using 5 μL 0.5% Nafion solution to prevent interference. The results obtained indicated that the effect of ascorbic acid to the xanthine response current of the enzyme electrodes was completely eliminated by the Nafion-coating.

3.10. Real sample analysis

The antiasthmatic drugs containing xanthine derivatives such as teophylline and aminophylline are used in the treatment of patients with respiratory distress syndrome. In the analysis of real samples, the two different drugs (1 and 2) were assayed to demonstrate the practical use of XO/Au/PVF/Pt and XO/Pt/PVF/Pt electrodes. The values measured for the xanthine determination and the recovery of the drug samples using both electrodes were summarized in Table 1. As can be seen, the values measured are satisfactory and agree closely with results given by the prospectuses of the drugs.

4. Conclusion

The development of new amperometric biosensors for monitoring xanthine was described in this paper. In our amperometric measurements, we observed that Au and Pt nanoparticles deposited on the PVF film have excellent catalytic activities towards the oxidation of H_2O_2. The xanthine biosensors, XO/Au/PVF/Pt and XO/Pt/PVF/Pt, exhibited also good analytical characteristics such as rapid response, high sensitivity, lower detection limit and good stability under the optimal conditions. Furthermore, the xanthine biosensors have satisfied performances in real sample measurements. These results may be attributed to the catalytic effect of Au and Pt nanoparticles and the compatibility of PVF film as a supporting material for the design of biosensors.

Acknowledgement

The authors are grateful for the financial support by the Scientific Research Projects (BAP-08101018) of Selcuk University.

References

[1] R. Hille, Arch. Biochem. Biophys. 433 (2005) 107–116.
[2] R. Harrison, Free Radic. Biol. Med. 33 (2002) 774–797.
[3] X. Liu, W.M. Lin, X.H. Yan, X.H. Chen, J.R. Hoidal, P. Xu, J. Chromatogr. B 785 (1998) 101–114.
[4] G. Berti, P. Fossati, G. Tarenghi, C. Musitelli, G.V. Melzid'Eril, J. Clin. Chem. Clin. Biochem. 26 (1988) 399–404.
[5] T. Richter, L.L. Shultz-Lockyear, R.D. Oleschuk, U. Bilitewski, D.J. Harrison, Sens. Actuators B 81 (2002) 369–376.
[6] E. Causse, A. Pradelles, B. Dirat, A. Negre-Salvayre, R. Salvayre, F. Couderc, Electrophoresis 28 (2007) 381–387.
[7] S. Renata, L. Pagliarussi, A.P. Luis, L. Freitas, J.K. Bastos, J. Sep. Sci. 25 (2002) 371–374.
[8] M. Czauderna, J. Kowalczyk, J. Chromatogr. B 744 (2000) 129–138.

[9] N. Cooper, R. Khosravan, C. Erdmann, J. Fiene, J.W. Lee, J. Chromatogr. B 837 (2006) 1–10.
[10] Ü.A. Kirgöz, S. Timur, J. Wang, A. Telefoncu, Electrochem. Commun. 6 (2004) 913–916.
[11] R. Villalonga, M. Matos, R. Cao, Electrochem. Commun. 9 (2007) 454–458.
[12] Y. Gao, C. Shen, J. Di, Y. Tu, Mater. Sci. Eng. C 29 (2009) 2213–2216.
[13] R. Devi, M. Thakur, C.S. Pundir, Biosens. Bioelectron. 26 (2011) 3420–3426.
[14] D. Shan, Y.N. Wang, H.G. Xue, S. Cosnier, S.N. Ding, Biosens. Bioelectron. 24 (2009) 3556–3561.
[15] D. Shan, Y. Wang, H. Xue, S. Cosnier, Sens. Actuators B 136 (2009) 510–515.
[16] D. Shan, Y. Wang, M. Zhu, H. Xue, S. Cosnier, C. Wang, Biosens. Bioelectron. 24 (2009) 1171–1176.
[17] K. Raju, K. Ajeet, P.R. Solanki, A.A. Ansari, M.K. Pandey, B.D. Malhotra, Anal. Chim. Acta 616 (2008) 207–213.
[18] C.H. Lee, S.C. Wang, C.J. Yuan, K.C. Chang, Biosens. Bioelectron. 22 (2007) 877–884.
[19] M. Pan, X. Guo, Q. Cai, G. Li, Y. Chen, Sens. Actuators B 108 (2003) 258–262.
[20] K. Takuya, O. Daisuke, K. Susumu, Electrochem. Commun. 9 (2007) 1012–1016.
[21] J. Xiaoyan, W. Yanhui, M. Xuyan, C. Xiujun, Z. Lainde, Sens. Actuators B 153 (2011) 158–163.
[22] Z. Wang, F.A. Xu, Q. Yang, J.H. Yu, W. Huang, Y. Zhao, Colloid Surf. B 76 (2010) 370–374.
[23] K.Y. Kwon, S.B. Yang, B.S. Kong, J. Kim, H.T. Jung, Carbon 48 (2010) 4504–4509.
[24] Y. Zou, C. Xiang, L. Sun, F. Xu, Biosens. Bioelectron. 23 (2008) 1010–1016.
[25] Y. Du, X. Luo, J.J. Xu, H.Y. Chen, Bioelectrochemistry 70 (2007) 342–347.
[26] X. Chu, D. Duan, G. Shen, R. Yu, Talanta 71 (2007) 2040–2047.
[27] W.S. Schlindwein, A. Kavvada, R.J. Latham, R.G. Linford, Polym. Int. 49 (2000) 953–959.
[28] L. Yu, M. Sahte, X. Zeng, J. Electrochem. Soc. 152 (2005) 357–363.
[29] H. Gülce, H. Özyörük, A. Yıldız, Ber. Bunsenges. Phys. Chem. 98 (1994) 228–233.
[30] H. Gülce, S.S. Çelebi, H. Özyörük, A. Yıldız, Pure Appl. Chem. 69 (1997) 173–177.
[31] H. Gülce, S.S. Çelebi, H. Özyörük, A. Yıldız, J. Electroanal. Chem. 394 (1995) 63–70.
[32] M. Kavanoz, H. Gülce, A. Yıldız, Turk. J. Chem. 28 (2004) 287–297.
[33] M.T. Sulak, Ö. Gökdoğan, A. Gülce, H. Gülce, Biosens. Bioelectron. 21 (2006) 1719–1726.
[34] T.W. Smith, J.E. Kuder, D. Wychick, J. Polym. Sci. 14 (1976) 2433–2448.
[35] D.D. Perrin, W.L.F. Armorego, Purification of Laboratory Chemicals, Pergamon Press, Oxford, 1980.
[36] P.J. Peerce, A.J. Bard, J. Electroanal. Chem. 112 (1980) 97–115.
[37] C. Qiong, P. Tuzhi, Y. Liju, Anal. Chim. Acta 369 (1998) 245–251.
[38] L. Mao, F. Xu, Q. Xu, L. Jin, Anal. Biochem. 292 (2001) 94–101.
[39] A. Rahman, M.S. Won, Y.B. Shim, Electroanalysis 19 (2007) 631–637.
[40] A.T. Lawal, S.B. Adeloju, J. Mol. Catal. B 66 (2010) 270–275.
[41] C.R. Raj, T. Okajima, T. Ohsaka, J. Electroanal. Chem. 543 (2003) 127–133.
[42] M. Çubukçu, S. Timur, Ü. Anik, Talanta 74 (2007) 434–439.
[43] H. Wu, J. Wang, X. Kang, C. Wang, D. Wang, J. Liu, I.A. Aksay, Y. Lin, Talanta 80 (2009) 403–406.
[44] J. Pei, X.Y. Li, Anal. Chim. Acta 414 (2000) 205–213.
[45] H.Y. Chen, R. Neeb, Fresenius J. Anal. Chem. 319 (1984) 240–247.
[46] F. Arslan, A. Yasar, F. Kılıç, Artif. Cells Blood Sub. 34 (2006) 113–128.
[47] F.R. Shu, G.S. Wilson, Anal. Chem. 48 (1976) 1679–1686.